ETHzürich

Pure and binary adsorption of CO2, H-2, and N-2 on activated carbon

Journal Article

Author(s):
Schell, Johanna; Casas, Nathalie; Pini, Ronny; Mazzotti, Marco

Pure and binary adsorption of CO_2, H_2, and N_2 on activated carbon

Johanna Schell · Nathalie Casas · Ronny Pini · Marco Mazzotti

Abstract A new developing field of application for pressure swing adsorption (PSA) processes is the capture of CO_2 to mitigate climate change, especially the separation of CO_2 and H_2 in a pre-combustion context. In this process scheme the conditions of the feed to the separation step, namely a pressure of 3.5 to 4.5 MPa and a CO_2 fraction of around 40% are favorable for an adsorption based separation process and make PSA a promising technology. Among the commercial adsorbent materials, activated carbon is most suitable for this application. To evaluate the potential, to benchmark new materials, and for process development a sound basis of the activated carbon thermodynamic data is required, namely equilibrium adsorption isotherms of the relevant pure components and mixtures, Henry's constants and isosteric heats.

In this work pure adsorption equilibria of CO_2, H_2 and N_2 on commercial activated carbon (AP3-60 from Chemviron, Germany) are measured using a Rubotherm Magnetic Suspension Balance (MSB) (Bochum, Germany) in a wide temperature and pressure range. The data is used to fit the temperature dependent parameters of Langmuir and Sips (Langmuir-Freundlich) isotherms and to determine the Henry's constants as well as isosteric heats. Based on this evaluation different methods to evaluate the data are compared and discussed. With the pure isotherm parameters of the Sips isotherm binary adsorption is predicted using an empirical binary Sips equation and ideal adsorbed solution theory (IAST). The results are compared to binary measurements in the same MSB applying a gravimetric-chromatographic method.

Notation

a	parameter for temperature dependent description of n_i^∞ [mmol/g]
A	specific surface of the adsorbent (Gibbs Adsorption isotherm) [m^2/kg]
A	parameter for temperature dependent description of k_i [1/MPa]
b	parameter for temperature dependent description of n_i^∞ [J/mol]
B	parameter for temperature dependent description of k_i [J/mol]
c	exponent in Sips isotherm [–]
C	parameter for temperature dependent description of H_i [mmol/g/MPa]
D	parameter for temperature dependent description of H_i [J/mol]
E	squared error from isotherm fitting [(mmol/g)^2]
g	weighting factor (final) [–]
H	Henry's constant [mmol/g/MPa]
ΔH	heat of adsorption [kJ/mol]
k	isotherm equilibrium constant [1/MPa]
m	mass [g]
M_1	weight at measuring point 1 [g]
M_1^0	weight at measuring point 1 under vacuum [g]
M	molar mass [g/mol]
n	molar adsorption per unit mass of adsorbent [mmol/g]
N	number of experimental data points at one temperature (one component) [–]

J. Schell · N. Casas · M. Mazzotti (✉)
Institute of Process Engineering, ETH Zurich, Sonneggstrasse 3, 8092 Zurich, Switzerland
e-mail: marco.mazzotti@ipe.mavt.ethz.ch

R. Pini
Department of Energy Resources Engineering, Stanford University, Stanford, USA

p	pressure [MPa]
r	weighting factor [–]
R	ideal gas constant [J/mol/K]
S	selectivity [–]
t	weighting factor [–]
T	Temperature [K]
V	Volume [cm^3]
V^0	Volume of lifted metal parts and adsorbent [cm^3]
V^{void}	Void volume of the adsorption system [cm^3]
V_2	second virial coefficient for isotherm description [g/mmol]
V_3	third virial coefficient for isotherm description [g^2/mmol^2]
w	mass fraction [–]
y	mole fraction in fluid [–]
z	mole fraction in adsorbed phase [–]

Greek letters

α	parameter for temperature dependent description of exponent c [–]
β	parameter for temperature dependent description of exponent c [–]
Π	spreading pressure [N/m]
ρ	molar density [mol/l]
ρ_m	mass density [g/l]

Sub- and superscripts

a	absolute adsorption, adsorbed phase
ads	adsorbent
calc	calculated value
ex	excess adsorption
exp	experimental value
feed	feed
i	component i
iso	isosteric
j	data point j
l	component l
ref	reference state for temperature dependent description of exponent c
s	adsorbed phase
tot	total
0	pure component (IAST), limiting heat
∞	saturation (isotherm equation)

Abbreviations

AC	activated carbon
GC	gas chromatography
IAST	ideal adsorbed solution theory
MSB	magnetic suspension balance
PSA	pressure swing adsorption
TGA	thermo gravimetric analysis

1 Introduction

The development of technologies to mitigate climate change is one of the big challenges today and in the future. One possibility to realize near-zero CO_2 emissions on a midterm timescale while keeping on using fossil fuels, for instance in power plants, is the so called concept of carbon capture and storage (CCS) (IPCC 2005). Applied at a power plant, a whole CCS system integrates the capture of the produced CO_2 at the power plant and its compression and transport to a location, where it is stored in such a way that it is separated from the atmosphere. With respect to the first step, three different strategies are under development, namely post-combustion capture, oxy-fuel combustion and pre-combustion capture. The latter is applied in an IGCC (integrated gasification combined cycle) power plant where the fuel, e.g. coal, is gasified and in a subsequent water-gas-shift (WGS) reactor converted to a mixture of mainly H_2 and CO_2. Additionally H_2O, N_2 and some impurities such as CO, H_2S and CH_4 might be present. Already at this point CO_2 is removed whereas H_2 is used for power generation. This technology can only be applied to newly built power plants, but in this case it provides several advantages. Especially the conditions of the feed to the separation step, namely a pressure of 3.5 to 4.5 MPa and a CO_2 fraction of around 40% are beneficial for the separation process. Due to these conditions a pressure swing adsorption (PSA) process looks very promising.

In order to evaluate the potential of a PSA process for CO_2 separation, commercial as well as new adsorbent materials have to be considered. As a first step towards this goal, studies aimed at the characterization of the adsorption equilibria are very useful. Knowing the equilibrium isotherms, already several important parameters of an adsorbent can be determined and its suitability for a specific application can be estimated (Hamon et al. 2010). Based on this information, possible improvements using new materials can be easily evaluated. An adsorbent for a pre-combustion CO_2 capture PSA process should exhibit in the first place a high adsorption capacity for CO_2 at pressures of around 1.5 to 2.0 MPa (corresponding to the partial pressure of CO_2 in the feed), a much lower adsorption capacity for H_2 and a low adsorption capacity of CO_2 at atmospheric pressure in order to prevent the need of vacuum for desorption of the CO_2 in the regeneration step. The first and the last requirement can be summarized in the need of a high cyclic working capacity in the operation pressure range also called delta loading (Hamon et al. 2010). Because of these specifications activated carbon is one of the most promising commercial materials as compared to adsorbents that show high loadings already at low (atmospheric) pressures, such as zeolites.

In this work the adsorption equilibria of pure CO_2, H_2 and N_2 and their binary mixtures on commercial activated

carbon (AP3-60 from Chemviron, Germany) are investigated. Pure component isotherms are measured in a Rubotherm Magnetic Suspension Balance (MSB) (Bochum, Germany) with in-situ density measurement. A wide pressure and temperature range is chosen to cover all possible and meaningful conditions for a pre-combustion CO_2 capture process. The data is described with Langmuir and Sips (Langmuir-Freundlich) isotherms by fitting the temperature dependent parameters to the experimental results. Furthermore, Henry's constants as well as isosteric heats are determined from the equilibrium data. With the Sips isotherm parameters of the pure components binary equilibria are predicted using an empirical extension of the pure isotherms as proposed by Ruthven (1994) on the one hand and ideal adsorbed solution theory (IAST) on the other hand. The predictive results are compared to binary measurements of CO_2/H_2 and CO_2/N_2 mixtures. These data are measured in the same MSB applying a gravimetric-chromatographic method. The results are discussed in particular with emphasis on their use for PSA in the context of pre-combustion CO_2 capture. N_2 adsorption is measured in this work for two reasons. First it is also present in the gas stream after the WGS reactor up to 4–5% and therefore needs to be considered in a final process design. Besides, N_2 is available in the whole IGCC CO_2 capture process scheme and could be used in some PSA process modifications which are not discussed in detail in this work.

2 Experimental

2.1 Materials

A commercial adsorbent, namely activated carbon AP 3-60 from Chemviron Carbon (Germany), is used in this study. The cylindrical pellets with a diameter of 3 mm are pretreated under vacuum at 150 °C for at least 8 hours before the experiments and the same procedure has been followed for intermediate regeneration between experiments. Independent TGA measurements confirmed that theses conditions are sufficient for drying and regeneration of the adsorbent.

Pure gases are obtained from Pangas (Dagmersellen, Switzerland) at purities of 99.9% for CO_2, 99.999% for H_2 and N_2 and 99.996% for He. For binary CO_2/H_2 and CO_2/N_2 measurements in each case three different mixtures are used with CO_2 molar fractions of 25%, 50% and 75%. The mixtures are produced by Pangas with relative errors of ±0.5 to 3% using the pure gases at purities of 99.995% for CO_2 and 99.996% for N_2 and H_2.

2.2 Measurements

Pure component adsorption isotherms are measured gravimetrically using a Rubotherm magnetic suspension balance

(MSB) (Rubotherm, Bochum, Germany). Most isotherms are measured in desorption mode, however, to rule out effects of hysteresis in some cases experiments in adsorption mode are performed and compared. For the determination of competitive mixture adsorption a gravimetric-chromatographic method is applied that uses the same MSB but extended with an in-house built circulation loop including additional adsorbent, a circulation pump that guarantees homogeneous mixing of the fluid phase and a sampling device for determination of the fluid phase composition at equilibrium by gas chromatography (GC). About 2 g and about 30 g of adsorbent are used for the pure and mixture isotherms, respectively. The experimental set-up was described in detail in previous publications (Ottiger et al. 2008; Pini et al. 2006). In the following, only the key equations in the evaluation of the experimental data are summarized.

Excess adsorption is the truly measurable quantity in an adsorption experiment, and it is defined as the difference between the absolute adsorbed mass m^a and the product of the bulk density ρ_m times the volume of the adsorbed phase V^a (buoyancy effect in a gravimetric experiment). In the pure component case the excess mass adsorbed is directly obtained from the gravimetric measurements as:

$$m^{ex}(\rho_m, T) = m^a - \rho_m V^a$$
$$= M_1(\rho_m, T) - M_1^0 + \rho_m V^0 \qquad (1)$$

where $M_1(\rho_m, T)$ and M_1^0 are the measured balance signals at the experimental conditions (ρ_m, T) and under vacuum, respectively. The last term on the right hand side accounts for the buoyancy of the adsorbent and the metal parts in the balance that is obtained by multiplying the bulk density ρ_m (in-situ measured by exploiting a calibrated titanium sinker) with the volume of these parts V^0 that was determined beforehand using Helium at conditions where it is assumed not to adsorb.

Special attention has to be paid in the case of H_2 adsorption. As H_2 adsorbs only in very small quantities and its molar mass is also small, the measured adsorption value is influenced strongly by uncertainties in M_1^0 and V^0. In order to minimize these uncertainties the values of M_1^0 and V^0 are determined newly before measuring each H_2 isotherm. By doing so, reproducible and consistent isotherms are measured in adsorption and desorption mode. Furthermore, the bulk density measured in-situ exhibits large fluctuation due to its low values in the case of H_2 adsorption. For this reason in the case of H_2, tabulated density values (NIST 2011) corresponding to the measured pressure and temperature are used instead.

In the case of binary adsorption (1) allows to determine only the total excess adsorption $m^{ex}(\rho^b, T) = m_1^{ex} + m_2^{ex}$. In order to distinguish between the two components, the gas

phase composition at equilibrium is measured by GC analysis and used in component mass balances:

$$m_i^{\text{ex}}(\rho_{\text{m}}, T) = w_i^{\text{feed}} m^{\text{feed}} - w_i \rho_{\text{m}} V^{\text{void}}, \quad i = 1, 2 \quad (2)$$

In this equation, V^{void} is the void volume of the whole system, which has to be determined prior to the experiments; w_i^{feed} and w_i are the mass fractions of the gas mixture in the feed and in the bulk at equilibrium conditions, respectively. The total amount of gas fed to the system m^{feed} is easily calculated as sum of the total excess m^{ex} and the total fluid mass in the void $m^{\text{fluid}} = \rho_{\text{m}} V^{\text{void}}$.

The excess mass adsorbed, calculated by (1) or (2), is converted to the molar excess adsorption per unit mass of adsorbent using the molar mass of component i, M_i, and the total mass of adsorbent in the experimental setup, m^{ads}:

$$n_i^{\text{ex}} = \frac{m_i^{\text{ex}}}{M_i m^{\text{ads}}} \quad (3)$$

To assure equilibrium conditions in the case of pure component isotherms, the equilibration time after each pressure change is at least three hours. Establishment of equilibrium is checked by monitoring all relevant parameters (pressure, temperature, density, M_1) until they show no more increase or decrease for at least 30 minutes. All values of one specific isotherm are measured in a row with evacuation of the instrument's chamber only between different isotherms. Repeated measurements using different equilibration times exhibit no difference, thus confirming that the procedure is correct.

In the case of binary adsorption, a trade off between equilibration time and possible selective leakage of one of the two gases out of the measurement chamber exists. It was observed that a waiting time of three hours after a change in pressure is enough to reach equilibrium and at the same time minimizes possible leakage. Binary adsorption can only be measured in adsorption mode in the used setup. Furthermore, in order to avoid error accumulation no more than two points are measured one after the other before the complete system is evacuated. To determine the gas composition at equilibrium five to seven independent GC measurements are performed and averaged.

3 Theory

3.1 Single component adsorption

3.1.1 Adsorption isotherm

The pure adsorption isotherms measured in this work are described with a Langmuir isotherm (Langmuir 1918) or a Sips (Langmuir-Freundlich) equation (Sips 1948; Do 1998) and by assuming a constant adsorbed phase molar density $\rho_i^{\text{a}} = n^{\text{a}}/V^{\text{a}}$. This is shown in the following equation:

$$
\begin{aligned}
n_i^{\text{ex}} &= n_i^{\text{a}} \left(1 - \frac{\rho}{\rho_i^{\text{a}}}\right) \\
&= \underbrace{\frac{n_i^{\infty} k_i p}{1 + k_i p}}_{\text{Langmuir equation}} \left(1 - \frac{\rho}{\rho_i^{\text{a}}}\right) \\
&= \underbrace{\frac{n_i^{\infty} (k_i p)^{c_i}}{1 + (k_i p)^{c_i}}}_{\text{Sips equation}} \left(1 - \frac{\rho}{\rho_i^{\text{a}}}\right)
\end{aligned}
\quad (4)
$$

where n_i^{ex} and n_i^{a} are the excess and absolute adsorption of component i at pressure p and bulk molar density ρ, respectively. For a pure component at a defined temperature, pressure p and density ρ in the fluid phase are directly related by an equation of state. Different methods to correlate excess and absolute adsorption are summarized elsewhere (Murata et al. 2001).

The Langmuir equation contains two parameters, namely the saturation capacity n_i^{∞} and the constant k_i. In the Sips equation there is a third parameter c_i ($0 < c_i \leq 1$) that accounts for the inhomogeneity of the adsorbent surface (Yang 1997; Sips 1948, 1950); the smaller c_i the less homogeneous is the surface. These parameters are determined for every temperature independently by fitting them to the experimental data. The values of the parameters are found by minimizing the weighted squared error E defined as:

$$E = \sum_{j=1}^{N} g_j \left(n_{\text{exp},j}^{\text{ex}} - n_{\text{calc},j}^{\text{ex}}\right)^2 \quad (5)$$

where N is the number of experimental data points measured for one isotherm and $n_{\text{exp},j}^{\text{ex}}$ and $n_{\text{calc},j}^{\text{ex}}$ are the experimental and calculated excess amounts adsorbed at this temperature for data point j, respectively; g_j is a weighting factor, which can be used to compensate for the inhomogeneous distribution of the experimental points as described in detail in Appendix.

The temperature dependence of the two parameters, n_i^{∞} and k_i, is described using an Arrhenius-type equation with parameters a_i and b_i, and A_i and B_i, respectively:

$$n_i^{\infty} = a_i \exp\left(\frac{-b_i}{RT}\right) \quad (6)$$

$$k_i = A_i \exp\left(\frac{-B_i}{RT}\right) \quad (7)$$

As no theoretically based relationship for the temperature dependence of parameter c is described in the literature (Do 1998) such dependence is obtained from the experimental results as discussed in more detail in Sect. 4.1.

3.1.2 Henry's constant

The Henry's constant, i.e. the slope of the tangent to the adsorption isotherm at $p = 0$, is an important characteristic of

adsorption since it gives an indication about the strength of adsorption and the isosteric heat of adsorption. In this work three different methods to obtain the Henry's constant are compared.

The most intuitive possibility is to fit the Henry's constant explicitly only to data measured in the low pressure region (method 1). Problems often arise using this method as many data points in the low p region are required, which is experimentally demanding. Additionally, these data at low p are especially error-prone. To avoid this, another method to determine the Henry's constant also using data at higher pressures is proposed in the literature (Zhou 2002; Ruthven 1984). It is based on the assumption that the adsorption data can be described with a virial isotherm (Ruthven 1984; Al-Muhtaseb and Ritter 1998; Taqvi and LeVan 1997a, 1997b):

$$\frac{H_i p}{n_i^{\mathrm{a}}} = \exp\left(2 V_{2,i} n_i^{\mathrm{a}} + \frac{2}{3} V_{3,i} (n_i^{\mathrm{a}})^2 + \cdots\right) \quad (8)$$

In the limit where $n_i^{\mathrm{a}} \to 0$, the series expansion can be cut after the second virial coefficient $V_{2,i}$. Assuming additionally that in this region because of the small buoyancy effect $n_i^{\mathrm{ex}} \approx n_i^{\mathrm{a}}$ holds, the following linear relationship is obtained:

$$\ln\left(\frac{p}{n_i^{\mathrm{ex}}}\right) = 2 V_{2,i} n_i^{\mathrm{ex}} - \ln H_i \quad (9)$$

This equation can be applied by using the experimental values to plot $\ln(p/n_i^{\mathrm{ex}})$ versus n_i^{ex}. The obtained curve exhibits a linear part, which can be extrapolated to intercept the vertical axis at $\ln H_i$; estimating the Henry's constant in this way is what we call method 2.

Evaluating the limit for $p \to 0$ of the Langmuir isotherm (4) shows that the product of the two parameters n_i^{∞} and k_i give exactly the Henry's constant (method 3). However, since these parameters are generally fitted to describe a wide pressure range, in most cases the agreement between model and experiment is not perfect in the low p region.

The temperature dependence of the Henry's constant H_i can be described in the same way as the one of the constant k_i, i.e. with an Arrhenius-type equation:

$$H_i = C_i \exp\left(\frac{-D_i}{RT}\right) \quad (10)$$

where the two parameters C_i and D_i are found by fitting the obtained values at the different temperatures. For method 3 this is only consistent if the saturation capacity n_i^{∞} and parameter k_i are both described with an Arrhenius-type equation or if the saturation capacity is temperature independent. In the latter case parameter D_i equals B_i (compare (7)).

3.1.3 Heat of adsorption

Adsorption, being exothermic, leads to changes in the temperature that can be significant and need to be taken into account when designing an adsorption-based separation process. These heat effects are best described using the isosteric heat of adsorption $\Delta H_i^{\mathrm{iso}}$, which can be determined already from the knowledge of the isotherms and defines the change in energy resulting from the phase change (gaseous phase to adsorbed phase) of an infinitesimal number of molecules at constant pressure p, temperature T and at a specific adsorbate loading n_i^{a}.

The Clausius Clapeyron equation (Sircar 1985; Zhou 2002) relates the isosteric heat to the change in pressure p of the bulk gas phase as a consequence of a change in the temperature T, while keeping the amount adsorbed n_i^{a} constant:

$$\Delta H_i^{\mathrm{iso}}(n_i^{\mathrm{a}}, T) = -R \left.\frac{\partial \ln p}{\partial (1/T)}\right|_{n_i^{\mathrm{a}}} \quad (11)$$

The use of this equation is based on the assumption that the gas bulk phase behaves in an ideal way and that the volume of the adsorbed phase can be neglected (Pan et al. 1998). Therefore it is only valid up to medium pressures.

Based on the experimental isotherms at different temperatures, the isosteric heat can be obtained by plotting $\ln(p)$ versus $1/T$ for a constant loading n_i^{a}. These points can usually be fitted with a straight line, whose slope is used in (11). This yields an isosteric heat that depends on loading but is averaged over temperature. However, this approach is questionable since isotherm values at the same loading for different temperatures are not easily available and linear interpolation does not always provide the right value. It can be circumvented by fitting the part of the isotherms relevant for evaluating the isosteric heat separately with a suitable isotherm equation and using these values as constructed "experimental" points. Furthermore, using the mathematical function describing the adsorption isotherm with temperature dependent parameters, an equation for the isosteric heat depending on loading and temperature can be readily derived from (11).

Applying the Clausius Clapeyron equation in the low pressure region, where the isotherm obeys the Henry's law, the limiting heat $\Delta H_i^{\mathrm{iso},0}$ is obtained directly from the temperature dependence of the Henry's constant (Sircar 1992):

$$\Delta H_i^{\mathrm{iso},0} = R \left.\frac{d \ln H_i}{d (1/T)}\right|_{n_i^{\mathrm{a}}} = -D_i \quad (12)$$

where the right hand side is obtained using (10). In this work, the isosteric heats obtained with the Clausius Clapeyron equation (11) using constructed "experimental" data and the Sips isotherm with the fitted temperature dependent parameters are compared to the limiting heat determined from the temperature dependence of the Henry's constants.

3.2 Binary adsorption isotherms

For practical applications, but also for theoretical considerations, predicting multicomponent adsorption from pure

component data is an important but challenging issue. Two approaches to obtain binary data based on the pure component isotherm parameters are considered in this work, namely one based on extending the pure isotherm equations empirically to binary isotherms and another that uses IAST (ideal adsorbed solution theory) to obtain the binary isotherms from the pure component isotherms. The results are compared to measured binary data.

To relate for component i in a mixture the experimental excess adsorption n_i^{ex} to the corresponding absolute adsorption n_i^a, a similar equation as for single component adsorption (see (4)) is used:

$$n_i^{ex} = n_i^a \left(1 - \frac{\rho y_i}{\rho^a z_i} \right) \quad (13)$$

ρ and y_i are the bulk phase density and mole fraction at equilibrium, respectively, whereas ρ^a and z_i are the density and mole fraction in the adsorbed phase. The density of the mixture adsorbed phase is obtained assuming ideal mixing and using the adsorbed phase densities of the individual components ρ_i^a (Sudibandriyo et al. 2003), i.e. for a binary mixture:

$$\frac{1}{\rho^a} = \frac{z_1}{\rho_1^a} + \frac{z_2}{\rho_2^a} \quad (14)$$

3.2.1 Empirical binary isotherms

An easy and often used possibility is the extended binary Langmuir equation:

$$n_i^a = \frac{n_i^\infty k_i y_i p}{1 + \sum_{l=1}^2 k_l y_l p} \quad (15)$$

In this equation the parameters obtained from the pure component case are used to build directly a competitive binary isotherm. A similar approach has been proposed for the Sips equation (Ruthven 1984):

$$n_i^a = \frac{n_i^\infty (k_i y_i p)^{c_i}}{1 + \sum_{l=1}^2 (k_l y_l p)^{c_l}} \quad (16)$$

Only for the binary Langmuir equation and in the case of equal saturation capacities n_i^∞, these binary isotherm equations are thermodynamically consistent. Nevertheless, in many cases a reasonably well description of the real behavior of the mixtures is provided with the main advantage of an explicit solution.

3.2.2 Ideal adsorbed solution theory

Another way to describe binary adsorption using the pure component parameters is the so called ideal adsorbed solution theory (IAST) (Myers and Prausnitz 1965). Similar to Raoult's law for vapor-liquid equilibrium in an ideal mixture the following phase equilibrium condition (isofugacity conditions) can be used:

$$p y_i = z_i p_i^0(T, \Pi) \quad (17)$$

where p is the pressure in the gas phase, y_i and z_i are the molar fractions of component i in the gas and adsorbed phase, respectively; $p_i^0(T, \Pi)$ is the pressure that pure component i would have in the bulk gas phase at the same temperature T and spreading pressure Π of the mixture.

Starting from the Gibbs adsorption isotherm a relation between the isotherm equation and the spreading pressure in the pure component case can be obtained (Ruthven 1984):

$$\int_0^{p_i^0} \frac{A}{RT} d\Pi = \int_0^{p_i^0} \frac{n_i^0(p_i)}{p_i} dp_i \quad (18)$$

where A is the specific surface of the adsorbent, Π is the spreading pressure, p_i is the partial pressure in the gas phase and $n_i^0(p_i)$ is the single component adsorption isotherm as given by (4). The integral on the left hand side is the same for all components. Using additionally the stoichiometric condition:

$$z_1 + z_2 = 1 \quad (19)$$

and the volume additivity in the adsorbed phase:

$$\frac{1}{n_{tot}} = \frac{z_1}{n_1^0(p_1)} + \frac{z_2}{n_2^0(p_2)} \quad (20)$$

the amounts adsorbed of each component can be calculated:

$$n_i^a = n_{tot} z_i \quad (21)$$

Only in the exceptional case where $n_1^\infty = n_2^\infty$ and $c_1 = c_2$ the equations can be solved analytically. For Langmuir isotherms the result is equivalent to the binary Langmuir equation (see (15)) in this case. Otherwise a system of nonlinear equations has to be solved numerically to find the solution. The advantage of this procedure is that a thermodynamically consistent description of the binary adsorption behavior is obtained.

4 Results

4.1 Single component adsorption

The experimental excess adsorption isotherms of pure CO_2, N_2 and H_2 on activated carbon at 25 °C, 45 °C, 65 °C, 100 °C and 140 °C versus the bulk density are shown as symbols in Fig. 1. The same symbols are used for the values measured in adsorption or desorption mode as no significant difference is observed between them. The temperatures are chosen in a way to cover the whole range of possible and reasonable conditions in a pre-combustion PSA process using activated carbon and the densities correspond to a wide range of pressures up to 20 MPa. The exact experimental pressure range for every isotherm is reported in Table 1. For the sake of clarity only experimental points at bulk densities $\rho > 0.5$ mol/l are plotted in Fig. 1, while the low density region ($\rho < 1$ mol/l) is shown in Fig. 2. At low pressures
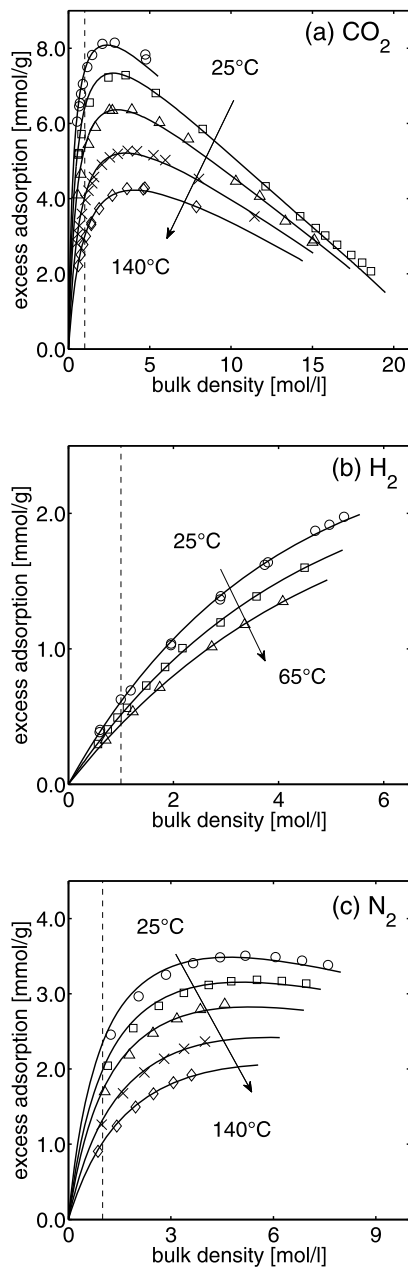
Fig. 1 Adsorption of pure CO_2 (**a**), H_2 (**b**) and N_2 (**c**) on activated carbon (*symbols*: experimental values; *lines*: fit with Langmuir isotherm assuming a constant density of the adsorbed phase) at different temperatures: 25 °C—circles, 45 °C—*squares*, 65 °C—*triangles*, 100 °C—*crosses*, 140 °C—*diamonds*; for clarity only points with bulk densities above 0.5 mol/l are shown, the low density region ($\rho \leq 1.0$ mol/l indicated by the *dashed vertical line*) is shown in Fig. 2; the corresponding experimental values are reported in the supplementary information

Fig. 2 Adsorption of pure CO_2 (**a**), H_2 (**b**) and N_2 (**c**) on activated carbon in the low density region ($\rho \leq 1.0$ mol/l) (*symbols*: experimental values; *lines*: fit with Langmuir isotherm assuming a constant density of the adsorbed phase) at different temperatures: 25 °C—circles, 45 °C—*squares*, 65 °C—*triangles*, 100 °C—*crosses*, 140 °C—*diamonds*; the corresponding experimental values are reported in the supplementary information

and for each species, the excess adsorbed amount increases monotonically with pressure. A gradual flattening with increasing pressure is observed for CO_2 and N_2, whereas the hydrogen isotherm is almost linear. At high pressure the situation is different and reflects the typical behavior of excess

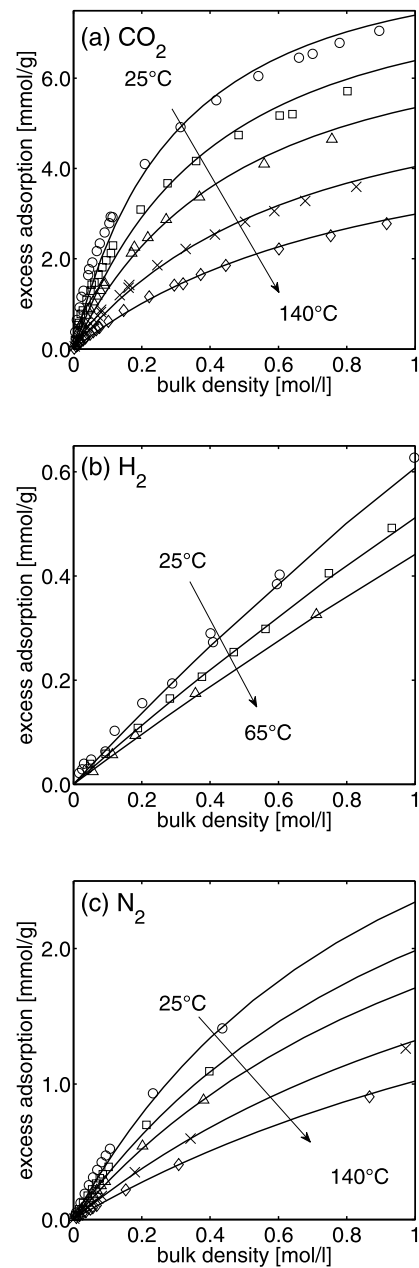adsorption isotherms measured at supercritical conditions. In the case of CO_2, adsorption increases with bulk density until a maximum value, which is followed by an almost linear decrease as density increases. For N_2 at 25 °C a maximum can still be observed, whereas at all other temperatures and for H_2, densities are too low to reach the region of decreasing excess adsorbed amounts.

Table 1 Overview of pure component and mixture equilibrium isotherm measurements on activated carbon; the mixture measurements are at 25 °C

	25 °C	45 °C	65 °C	100 °C	140 °C
CO_2	0.01–7.1 MPa	0.01–21.0 MPa	0.01–18.9 MPa	0.01–21.2 MPa	0.01–20.1 MPa
H_2	0.04–14.1 MPa	0.13–12.8 MPa	0.16–12.2 MPa	–	–
N_2	0.006–19.9 MPa	0.01–19.6 MPa	0.008–13.4 MPa	0.005–13.0 MPa	0.03–13.1 MPa
$y_{CO_2}^{Feed}$		0.25		0.50	0.75
H_2/CO_2		1.2–11.8 MPa		1.7–10.2 MPa	0.4–10.8 MPa
N_2/CO_2		1.0–6.0 MPa		1.0–6.0 MPa	0.8–6.1 MPa

The experimental data is summarized in the supplementary information and is used to fit the parameters of Langmuir and Sips isotherms as explained in Sect. 3.1.1. For this purpose, a constant density of the adsorbed phase was assumed and set to be equal to the liquid density of the adsorbate at specific conditions. Such conditions have been chosen in order to allow for the best fitting of the experimental data and at the same time to be consistent with previous studies. Specifically, the density values are 23 mol/l for CO_2 (corresponding to 18.0 MPa and 0 °C: NIST 2011; Sudibandriyo et al. 2003; Humayun and Tomasko 2000), 35 mol/l for H_2 (corresponding to 0.1 MPa and 20.3 K, i.e. boiling point, NIST 2011; Grande et al. 2008) and 29 mol/l for N_2 (corresponding to 0.1 MPa and 77.3 K, i.e. boiling point, NIST 2011; Grande et al. 2008; Dreisbach et al. 1999). In the case of a Langmuir isotherm, the results of this fitting are illustrated by the curves in Figs. 1 and 2. In the same way the results of the fitting in the case of Sips isotherms are shown in Figs. 3 and 4, whereas all fitted parameters are reported in Tables 2 and 3.

For all three gases and at all temperatures the Langmuir isotherm can describe the experimental values reasonably well, especially in the region of higher bulk densities. However at very low densities the adsorption is somewhat underestimated by the fitted Langmuir isotherms as compared to the experimental values. The fitting of the Sips equation shows a different picture. Considering the whole experimental density range, the fits look equally well (compare Figs. 1 and 3), in the low density region (see Figs. 2 and 4), however, the experimental points are much better described by the Sips model than by the Langmuir isotherm. This indicates that the Sips isotherm, that accounts for a non-uniform distribution of surface energy, is more suitable to describe the behavior especially in the low density region.

This inhomogeneity of the adsorbent surface is described by the parameter c_i in the Sips isotherm equation, with $0 < c_i \leq 1$. For a value of $c_i = 1$ again the Langmuir isotherm with a completely homogeneous surface is obtained whereas the smaller c_i the bigger the degree of inhomogeneity (Sips 1948). No theoretical thermodynamic dependence of c_i on the temperature is discussed in the literature (Do 1998). In this work no clear temperature dependence of c_i is obtained

in the case of H_2 and N_2 adsorption. Therefore an average value of the first fitting is calculated and kept constant during a second fitting of the temperature dependent parameters. For CO_2 adsorption a S-shaped increase in c_i with temperature is observed and described with the following empirical functional form:

$$c_i = \alpha_i \, \text{atan} \left(\beta_i \left(T - T_{\text{ref},i} \right) \right) + c_{\text{ref},i} \qquad (22)$$

To describe the temperature dependence of the other parameters of the Sips isotherm and the one of the Langmuir isotherm, i.e. n_i^∞ and k_i, Arrhenius type equations (6) and (7) are used. In principle n_i^∞ should not exhibit any temperature dependence; however, with a constant value the experimental values can not be described satisfactory, except for H_2. In this case no temperature dependence of $n_{H_2}^\infty$ is observed, therefore b_{H_2} in (6) equals zero. Again as in the case of non-temperature dependent c_i values, an average value of $n_{H_2}^\infty$ is calculated after the first fitting and kept constant during a second fitting of k_{H_2}. The values of all parameters a_i, b_i, A_i, B_i, α_i, β_i, $T_{\text{ref},i}$ and $c_{\text{ref},i}$ are given in Table 4.

Using the experimental excess data, the Henry's constants are calculated by all methods explained in Sect. 3.1.2. In Fig. 5, the results are shown in form of $\ln(H_i)$ versus $1/T$. The exact values obtained for CO_2, N_2 and H_2 at all temperatures with all three methods are summarized in the supplementary information. For method 1 (direct fit in the linear low p region) the isotherms up to pressures of 0.05 MPa or 0.3 MPa for CO_2 and N_2 or H_2 are used, respectively. It is obvious that these values (represented by the circles) and the ones obtained by method 2 (using a virial type isotherm represented by the triangle) are mostly in good agreement, whereas the value obtained with method 3 (from Langmuir parameters, squares) are slightly smaller, except for H_2, where all values coincide rather well. This corresponds to the fact that the adsorption at low densities is somewhat underestimated by the Langmuir isotherm, as reflected exactly by the values obtained using method 3 (see Fig. 2). Therefore for further evaluation only the values obtained with methods 1 and 2 are used and combined into a single set of values. Comparing the values for the different adsorbates, CO_2 shows the highest Henry's constants, which indicates the strongest adsorption in the low p region, fol-
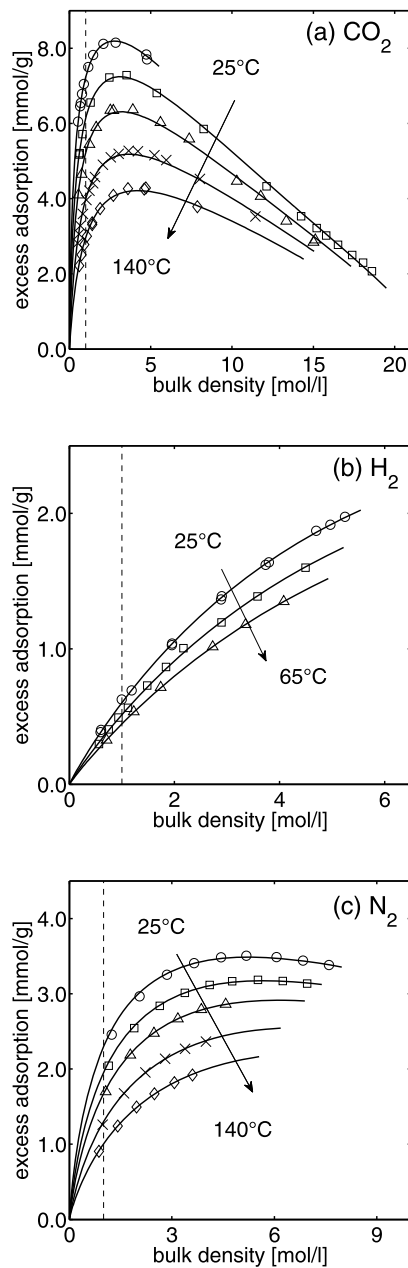
Fig. 3 Adsorption of pure CO_2 (**a**), H_2 (**b**) and N_2 (**c**) on activated carbon (*symbols*: experimental values; *lines*: fit with Sips isotherm assuming a constant density of the adsorbed phase) at different temperatures: 25 °C—*circles*, 45 °C—*squares*, 65 °C—*triangles*, 100 °C—*crosses*, 140 °C—*diamonds*; for clarity only points with bulk densities above 0.5 mol/l are shown, the low density region ($\rho \leq 1.0$ mol/l indicated by the *dashed vertical line*) is shown in Fig. 2; the corresponding experimental values are reported in the supplementary information

Fig. 4 Adsorption of pure CO_2 (**a**), H_2 (**b**) and N_2 (**c**) on activated carbon in the low density region ($\rho \leq 1.0$ mol/l) (*symbols*: experimental values; *lines*: fit with Sips isotherm assuming a constant density of the adsorbed phase) at different temperatures: 25 °C—*circles*, 45 °C—*squares*, 65 °C—*triangles*, 100 °C—*crosses*, 140 °C—*diamonds*; the corresponding experimental values are reported in the supplementary information

lowed by N_2 and H_2. As indicated by the linear behavior in Fig. 5, the temperature dependence of the Henry's constants for all components can be well described with an Arrhenius type equation (10) using the parameters reported in Table 5.

In the Henry region, i.e. for $p \rightarrow 0$ and small amounts adsorbed, the limiting heat of adsorption equals the param-
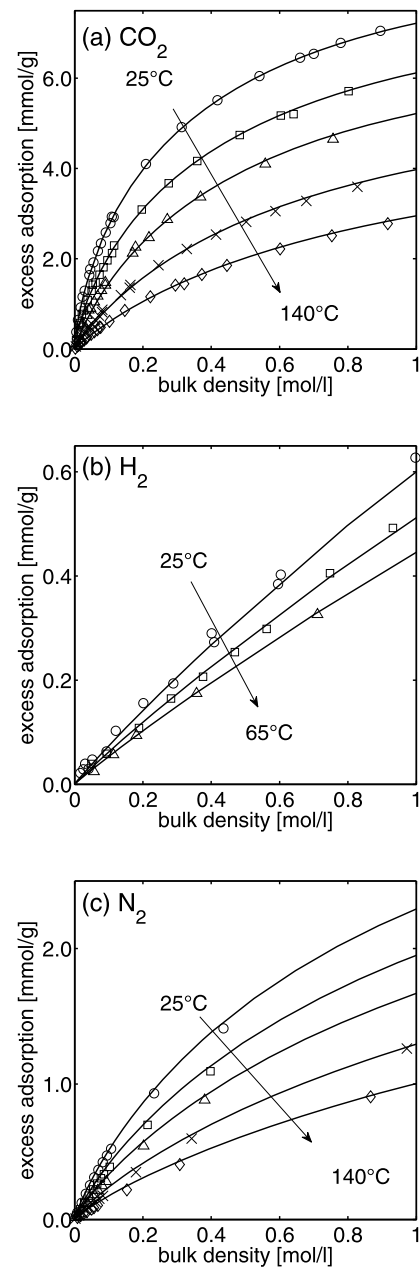
eters $-D_i$ in the temperature dependent description of the Henry's constants (compare (10) and (12)). For higher loadings the Clausius Clapeyron equation is used for every component to calculate the isosteric heat using constructed "experimental" data (compare Sect. 3.1.3) or the Sips isotherm with the temperature dependence of the parameters resulting in the following equation:

Table 2 Langmuir parameters for the adsorption of pure components on activated carbon at different temperatures

	25 °C	45 °C	65 °C	100 °C	140 °C
CO_2					
n_i^∞ [mmol/g]	10.83	10.33	9.21	8.00	6.88
k_i [1/MPa]	1.142	0.771	0.603	0.387	0.256
E	4.66×10^{-2}	2.83×10^{-2}	1.24×10^{-2}	6.29×10^{-3}	2.51×10^{-3}
H_2					
n_i^∞ [mmol/g]	5.35	5.35	5.35	–	–
k_i [1/MPa]	0.053	0.041	0.033	–	–
E	3.37×10^{-4}	6.84×10^{-5}	2.10×10^{-5}	–	–
N_2					
n_i^∞ [mmol/g]	5.14	4.80	4.38	3.94	3.52
k_i [1/MPa]	0.363	0.283	0.241	0.170	0.124
E	5.63×10^{-3}	3.54×10^{-3}	2.00×10^{-3}	6.57×10^{-4}	2.91×10^{-4}

Table 3 Sips parameters for the adsorption of pure components on activated carbon at different temperatures

	25 °C	45 °C	65 °C	100 °C	140 °C
CO_2					
n_i^∞ [mmol/g]	13.27	12.11	9.85	8.38	7.22
k_i [1/MPa]	0.666	0.488	0.498	0.340	0.225
c_i [–]	0.74	0.77	0.88	0.93	0.94
E	5.01×10^{-4}	3.06×10^{-3}	6.35×10^{-3}	4.24×10^{-3}	1.43×10^{-3}
H_2					
n_i^∞ [mmol/g]	6.66	6.66	6.66	–	–
k_i [1/MPa]	0.037	0.029	0.023	–	–
c_i [–]	0.96	0.96	0.96	–	–
E	1.33×10^{-4}	9.05×10^{-5}	7.18×10^{-6}	–	–
N_2					
n_i^∞ [mmol/g]	5.64	5.36	5.15	4.89	4.64
k_i [1/MPa]	0.280	0.212	0.161	0.104	0.068
c_i [–]	0.86	0.86	0.86	0.86	0.86
E	6.97×10^{-4}	2.64×10^{-4}	1.41×10^{-4}	8.82×10^{-5}	7.54×10^{-5}

Table 4 Parameters to describe the Langmuir and Sips isotherms temperature dependent; the temperature dependences of n_i^∞ and k_i are both described with an Arrhenius type equation, whereas the temperature dependence of c_{CO_2} is described with an inverse tangent. No temperature dependence is observed for n_i^∞ in the case of H_2 adsorption and for c_i in the case of N_2 and H_2 adsorption

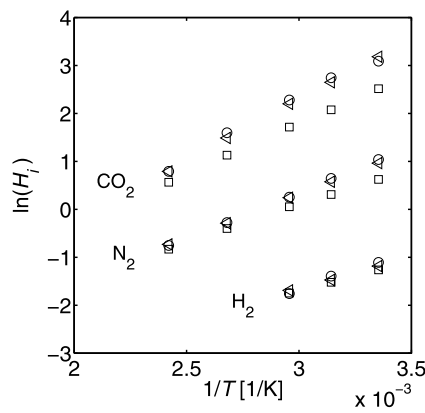|		CO_2	H_2	N_2
Langmuir				
n_i^∞ [mmol/g]	a_i [mmol/g]	2.07	5.35	1.31
	b_i [J/mol]	−4175	0	−3407
k_i [1/MPa]	A_i [1/MPa]	5.59×10^{-3}	8.76×10^{-4}	7.83×10^{-3}
	B_i [J/mol]	−13133	−10162	−9535
Sips				
n_i^∞ [mmol/g]	a_i [mmol/g]	1.38	6.66	2.82
	b_i [J/mol]	−5628	0	−1706
k_i [1/MPa]	A_i [1/MPa]	1.68×10^{-2}	6.97×10^{-4}	1.74×10^{-3}
	B_i [J/mol]	−9159	−9826	−12661
c_i [–]	α_i [–]	0.072	0	0
	β_i [1/K]	0.106	0	0
	$c_{ref,i}$ [–]	0.83	0.96	0.86
	$T_{ref,i}$ [K]	329	273	273

Fig. 5 Henry's constants for all three components CO_2, N_2 and H_2 in the form $\ln(H_i)$ versus $1/T$. The values are obtained by the three different methods, namely (1) linear fit to low p exp. data (*circle*), (2) using a Virial type isotherm equation (*triangle*), (3) from Langmuir parameters (*squares*)

Table 5 Parameters to describe the temperature dependence of the Henry's constants; the temperature dependence is fitted to an Arrhenius type equation

	C_i [mmol/g/MPa]	D_i [J/mol]
CO_2	5.27×10^{-3}	-20931
H_2	2.45×10^{-3}	-12079
N_2	5.00×10^{-3}	-15610

$$
\begin{aligned}
\Delta H_i^{\text{iso}} = & -B_i \\
& - \frac{b_i}{c_i(T)} \left(\frac{n_i^\infty(T)}{n_i^\infty(T) - n_i^{\text{a}}} \right) \\
& - \frac{RT^2 \alpha_i \beta_i}{c_i(T)^2 (1 + \beta_i^2 (T - T_{\text{ref},i})^2)} \\
& \times \ln \left(\frac{n_i^{\text{a}}}{n_i^\infty(T) - n_i^{\text{a}}} \right)
\end{aligned}
\tag{23}
$$

For CO_2 the highest amount adsorbed that is evaluated is 4 mmol/g, whereas for N_2 only values up to 2 mmol/g and for H_2 only values up to 1 mmol/g are considered in order to consider conditions that are consistent with the assumptions detailed in Sect. 3.1.3. Consequently, only this part of the isotherm was used to obtain the constructed "experimental" data. Because the Langmuir isotherm does not describe the experimental data very well in this low pressure region, it was not used in the evaluation. A comparison of the results determined for the isosteric heat as a function of the amount adsorbed at different temperatures is illustrated in Fig. 6.

For the three components a different behavior can be observed resulting directly from the temperature dependence of the isotherms. The isosteric heat obtained by (23) is independent of loading n^{a} and temperature if the saturation capacity n_i^∞ and also the exponent c_i are independent of temperature, i.e. $b_i = \alpha_i = 0$. This is reflected in the constant
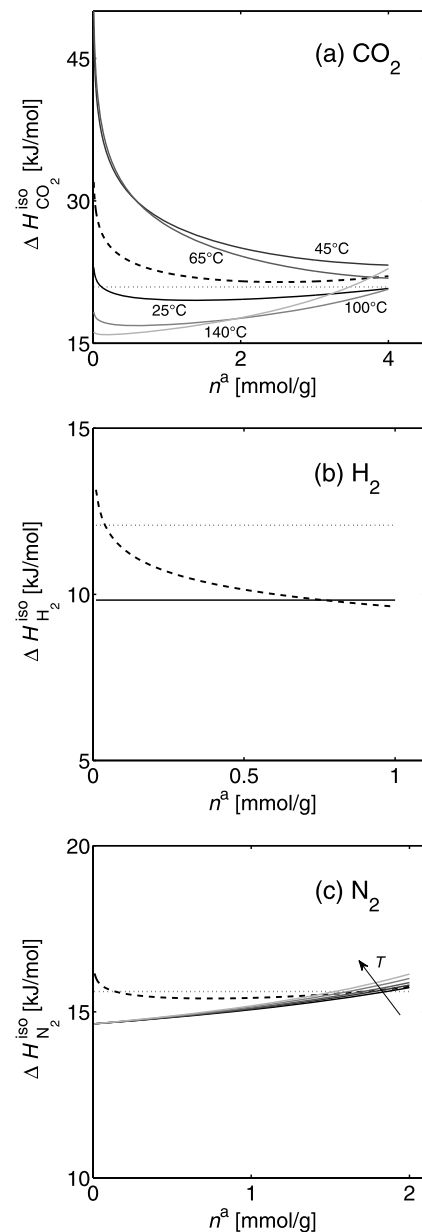

Fig. 6 Isosteric heat of adsorption for pure CO_2 (**a**), H_2 (**b**) and N_2 (**c**) on activated carbon dependent on the amount adsorbed as obtained by the Clausius Clapeyron equation; *dashed lines* give the results obtained from constructed "experimental" data (averaged over temperature) whereas *solid lines* show the result using the temperature dependent Sips isotherms; the same temperatures as for the isotherm measurements are plotted, namely 25 °C, 45 °C, 65 °C, 100 °C and 140 °C, the lower the temperature the darker the line; *dotted lines* represent the value of the limiting heat that is given by the temperature dependence of the Henry's constants

value of the isosteric heat of H_2. The values of $\Delta H_{H_2}^{\text{iso}}$ equal the parameter $-B_{H_2}$ in the temperature dependent description of the isotherm parameter k_{H_2} (in the Sips isotherm). The value obtained from the temperature dependence of the Henry's constant is slightly higher, whereas the isosteric heat derived from the constructed "experimental" values lies

in between. At low loading it is close to the limiting heat and approaches the value calculated with (23) at higher loadings. In the case of N_2 with a temperature independent exponent c_i but a saturation capacity n_i^∞ dependent on temperature, (23) gives an isosteric heat which is dependent on temperature and increases with loading, shown in Fig. 6(c). At low loadings the limiting heat and the isosteric heat calculated from the constructed "experimental" values have a slightly higher value as compared to the values calculated with (23). If both, the saturation capacity n_i^∞ and also the exponent c_i are dependent on temperature, apart from the constant $-B_i$, two terms in (23) determine the temperature and loading dependent behavior of the isosteric heat. This is the case for CO_2, shown in Fig. 6(a). The first term is increasing with increasing loading as seen already for N_2, whereas the second term decreases with increasing loading. This second term becomes especially important for $n_i^a \to 0$, due to the presence of the logarithm that makes the isosteric heat diverge. The big difference between the temperatures in the case of CO_2 can be explained by the temperature dependence of the exponent c_i which is included in the factor before the logarithm in (23).

This discussion shows that the value obtained for the isosteric heat by using the Clausius Clapeyron equation is very sensitive to the isotherm description used in the evaluation. From an application point of view, e.g. when designing an adsorption-based process, in most cases an average value that represents the relevant temperatures and loadings is suitable for the description. Independent of this loading and temperature dependent behavior a clear trend is observed from CO_2 having the highest isosteric heat to N_2 and H_2 with the lowest value, i.e. the same trend as observed for adsorption capacity and strength.

4.2 Binary adsorption

An overview of the conditions (pressure and composition of the feed mixture) for the binary CO_2/H_2 and CO_2/N_2 experiments at 25 °C is given in Table 1. However, due to the selective adsorption of CO_2, the bulk composition at equilibrium is different from the feed composition and different for every experimental point as already discussed in detail elsewhere (Ottiger et al. 2008). All measured excess adsorption data are converted to absolute amounts by using (13) and (14), the latter describing the total adsorbed phase density as a weighted average of the single component adsorbed phase densities, given in Sect. 4.1 based on the volume additivity of an ideal mixture.

It is known that for predicting binary adsorption from the pure component isotherms using IAST especially the accuracy in the low pressure region is important (Gamba et al. 1989). As this region is described significantly better by the Sips isotherms, in the following only binary predictions based on the pure component Sips isotherms are considered,
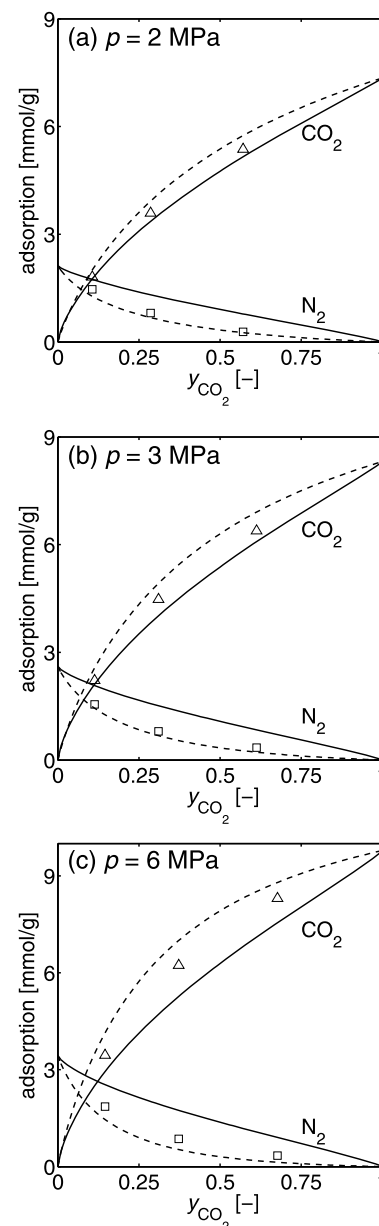

Fig. 7 Binary adsorption equilibria (absolute adsorption) of CO_2 (*triangles*) and N_2 (*squares*) on activated carbon at 25 °C and at three different pressures; *Symbols*: experimental results, *solid lines*: binary Sips calculation using pure component parameters, *dashed lines*: IAST calculation using pure component parameters (Sips); the corresponding data are reported in the supplementary information

unless stated differently. For CO_2/N_2 mixtures the absolute adsorption data obtained at three different pressures (2, 3 and 6 MPa) is shown in Fig. 7 together with the predictive results from the binary Sips and IAST calculation using the single component Sips parameters. As expected from the single component results, CO_2 is the heavy, that is more adsorbed, component. As a consequence, N_2 is enriched in the bulk and the measured CO_2 equilibrium compositions are shifted towards lower values as compared to the feed

composition. For all three pressures and at all bulk compositions, the trend of adsorption can be well described with both the empirically extended binary Sips and IAST. However, IAST predicts the measured values quantitatively better, which could be caused by the thermodynamic consistent description of the competitive behavior of the two components. Moreover, the higher the pressure the bigger is the difference between the two models, with IAST consistently predicting a higher adsorption of CO_2 and a lower adsorption of N_2 compared to binary Sips except for very low CO_2 bulk mole fractions.

For CO_2/H_2 mixtures the same evaluation is done at three different pressures, namely for 2, 3 and 8 MPa as shown in Fig. 8. Again, CO_2 adsorbs preferentially as compared to H_2, this trend being well predicted by the two models. For all three pressures and at all bulk compositions, the adsorption of CO_2 can be quantitatively well described with both binary Sips and IAST using the pure component Sips parameters. At lower pressures (2 and 3 MPa), hardly any difference between the two calculations is observed, while at high pressure IAST predicts a slightly higher adsorption of CO_2 and lower adsorption of H_2 when compared to the binary Sips case. Considering H_2 adsorption, it is evident how the difference between experimental and predicted H_2 values increases with increasing H_2 concentration in the bulk. At high H_2 concentration in the bulk and for all pressures the experimental values are larger than the prediction. This could indeed reflect the fact that H_2 is more adsorbed than predicted by the models, but it could also result from the difficulty to measure H_2 adsorption. This issue is further analyzed and discussed in Sect. 5.

A comparison between predicted binary adsorption based on pure Sips and Langmuir isotherms is shown in Fig. 9 for the case of CO_2/H_2 mixtures adsorption at 25 °C and 3 MPa. The prediction was done by IAST using the pure component isotherm parameters from the Sips (solid line) and Langmuir (dashed line) equation. In both cases the qualitative behavior from the experiments (shown as symbols) is well predicted by the models, however, as anticipated, the prediction using the pure component Sips isotherm is quantitatively better. This can be seen for instance in the prediction of the CO_2 adsorption. Using the Langmuir isotherms the CO_2 adsorption is slightly underestimated at low CO_2 bulk mole fractions whereas it is overestimated at high CO_2 bulk mole fraction compared to the experimental points. Using the pure component Sips isotherms the CO_2 adsorption at all three experimental bulk mole fractions is well predicted. All data is provided as Supplementary Information.

5 Discussion

Considering the single component adsorption and comparing the adsorption capacity of the three gases, it is clear
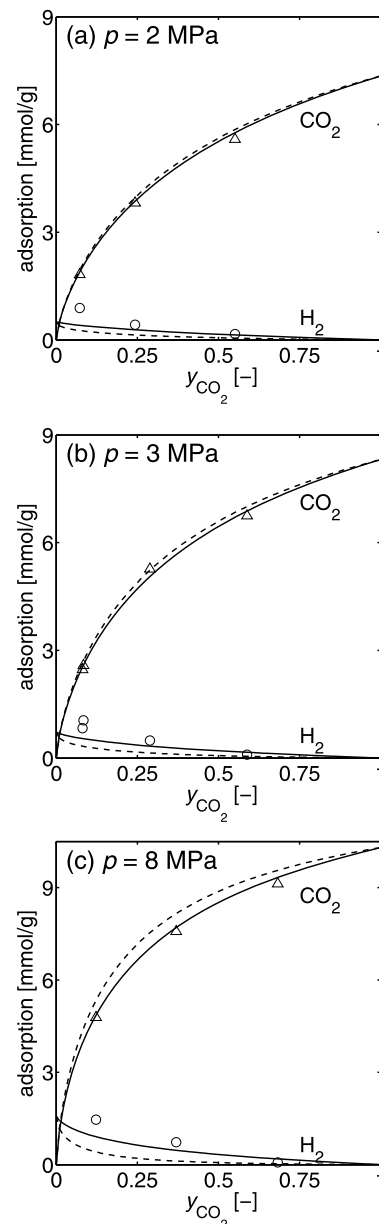

Fig. 8 Binary adsorption equilibria (absolute adsorption) of CO_2 (*triangles*) and H_2 (*circles*) on activated carbon at 25 °C and at three different pressures; *Symbols*: experimental results, *solid lines*: binary Sips calculation using pure component parameters, *dashed lines*: IAST calculation using pure component parameters (Sips); the corresponding data are reported in the supplementary information

that CO_2 is adsorbed significantly more than N_2, which in turn is more adsorbed than H_2, as expected. The exact values of the adsorbed amount depend on the type of activated carbon, as well as on the preparation and activation procedure. However, when comparing the values of the pure component isotherms presented in this paper with results measured on comparable materials, the adsorbed amounts agree quite well and show the same trends (Hwang et al. 1991; Park et al. 1998; Humayun and Tomasko 2000; Sudiban-
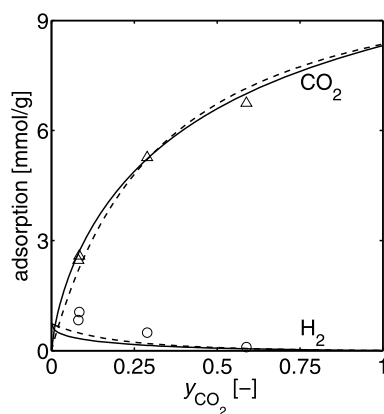
Fig. 9 Comparison of the binary adsorption of CO_2 (*triangles*) and H_2 (*circles*) on activated carbon at 25 °C and 3.0 MPa predicted by IAST with the isotherm parameters of the pure Langmuir or Sips isotherms; *Symbols*: experimental results, *solid lines*: Sips IAST, *dashed lines*: Langmuir IAST
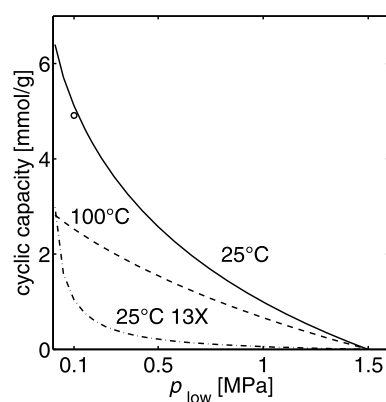

Fig. 10 Cyclic working capacities between a high adsorption pressure of 1.5 MPa and different low desorption pressures p_{low} for CO_2 on activated carbon AP3-60 at 25 °C and 100 °C based on the pure component Sips isotherms; additionally one point taking into account competition between H_2 and CO_2 during adsorption is shown (*circle*); for comparison the values for zeolite 13X at 25 °C are shown as reported by Xiao et al. (2008)

driyo et al. 2003; Shen et al. 2010; Grande et al. 2008; Lopes et al. 2009). Consequently, the activated carbon adsorbent seems to be suitable for the separation of CO_2/H_2 mixtures by a pressure swing adsorption (PSA) process.

However, for the use of an adsorbent in such a process, not only the absolute capacity is decisive, but also the regeneration behavior. Especially in the application of precombustion CO_2 capture the energy penalty of the process is crucial and influenced, among others, by the CO_2 desorption pressure, due to the following CO_2 compression to 10.0–15.0 MPa for transportation and storage, and by the process temperature. Therefore the cyclic working capacity, also called delta loading (Hamon et al. 2010), which is the change in the adsorbed amount between a high adsorption pressure and the possible desorption pressure, plays a key role. In a first step this cyclic capacity can be evaluated based on the pure component isotherm, assuming that the absolute value is indeed affected by the competitive behavior, but its shape is not. This will be especially true for CO_2 in the case of CO_2/H_2 adsorption as H_2 is significantly less adsorbed. In this way the cyclic capacity is a useful tool to check the potential of an adsorbent for a specific application at an early stage and to compare different materials.

For CO_2 the cyclic working capacity at 25 °C and 100 °C is shown in Fig. 10 versus different desorption pressures keeping constant the adsorption pressure at 1.5 MPa, which corresponds approximately to the CO_2 partial pressure in a pre-combustion feed to the PSA unit. For comparison, the cyclic working capacity of zeolite 13X at 25 °C is also plotted in the same figure where the zeolite isotherm data are taken from Xiao et al. (2008). The low values for 13X show clearly that zeolites are no suitable option in the case of precombustion CO_2 capture.

Moreover, one point referring to the competitive CO_2/H_2 mixture behavior is shown in Fig. 10 as a circle. The fol-

Table 6 Cyclic working capacities [mmol/g] for CO_2 adsorption on activated carbon based on the pure component Sips isotherm; the pressure is cycled between 1.5 MPa as high adsorption pressure and different low desorption pressures p_{low}

p_{low} [MPa]	25 °C	45 °C	65 °C	100 °C	140 °C
0.1	5.2	4.2	3.6	2.5	1.8
0.2	4.3	3.5	3.1	2.3	1.6
0.5	2.6	2.2	2.1	1.6	1.1

lowing assumptions are used in the calculation of the cyclic adsorption capacity for this point: feed at 25 °C and 3.0 MPa with an equimolar mixture of CO_2 and H_2; the adsorption is calculated with the binary Sips isotherm whereas the desorption takes place at 0.1 MPa at pure CO_2 conditions. It is clear that the CO_2 cyclic capacity is only influenced in a minor way by the presence of H_2, thus justifying the use of pure isotherms for a first assessment.

Values for pure CO_2 at different temperatures and three selected desorption pressures are reported in Table 6. It is obvious that the cyclic working capacity decreases with increasing temperature or increasing desorption pressure. This results in a trade-off between process temperature, desorption pressure and cyclic working capacity, which has to be optimized by a proper process development taking into account additionally the competitive effects as well as kinetics, heat and mass transfer phenomena. Nevertheless, the values reported give a good indication about the process performance and can be used to compare different adsorbent materials.

Apart from the cycling working capacity of the pure components, the mixture behavior is also important. In many cases the aim is to express it as a function of the single

Table 7 H_2 and CO_2 excess adsorption with the assumption of different selective H_2 leakages; the experimental point is specified by the following conditions: CO_2 molar fraction in the feed of 25%, H_2 molar fraction in the feed of 75%, 3.0 MPa, 25 °C, CO_2 mass fraction in the bulk at equilibrium of 65.8%

Assumed H_2 leakage	$n_{H_2}^{ex}$ [mmol/g]	$n_{CO_2}^{ex}$ [mmol/g]
0%	0.69	2.45
5%	0.26	2.47
15%	−0.61	2.51

component parameters. Binary or multicomponent measurements are only used for comparison and confirmation as it is done in this work (compare Sect. 4.2). Observed deviations between measurements and prediction as for instance in the adsorption of H_2 (see Fig. 8) have to be discussed and justified if the predictive calculations are further used. In this work the deviations in the H_2 adsorption in the binary experiments could be caused on the one hand by a different adsorption mechanism, i.e. H_2 adsorption is not decreased by the competitive co-adsorption of CO_2 but possibly even enhanced. However, this would not explain why the deviations are larger for higher H_2 mole fractions. On the other hand, the deviations could be caused by an error in the measured data. One possibility in our experimental set-up is a selective leakage of H_2 out of the system, which would yield a deviation in the observed direction. During the experiments leakage of H_2 was detected but not quantified. Moreover points measured after different equilibration times showed no clear trend.

This uncertainty is particularly important in the case of H_2 as it has a molar weight of only 2 mol/g. Therefore, a small error in the mass balance leads to a larger deviation in terms of adsorption expressed in moles of adsorbate per unit mass of adsorbent. In order to show its impact, this effect is evaluated exemplarily for one point under the following conditions: CO_2 molar fraction in the feed of 25%, H_2 molar fraction in the feed of 75%, 3.0 MPa, 25 °C, CO_2 mass fraction in the bulk at equilibrium of 65.8%. Three different cases are assumed in the evaluation of the experimental data: no leakage, 5% selective H_2 leakage and 15% selective H_2 leakage. The results for the H_2 and CO_2 excess are summarized in Table 7. It can be seen that already the assumption of a small H_2 leakage results in a significant deviation in the H_2 excess, although nearly no effect on the CO_2 excess is observed.

On the other hand, the competitive behavior of CO_2/N_2 mixtures can be well predicted by IAST using the pure component Sips isotherms (compare Fig. 7). Furthermore, the CO_2/N_2 system excludes all experimental difficulties associated with the measurement of H_2, but can be assumed to behave similarly to CO_2/H_2. Hence, it can be concluded that IAST using the pure component Sips parameters should be

able to predict CO_2/H_2 mixture adsorption equally well being more reliable in the case of H_2 adsorption than the experimental measurements.

The competitive behavior in binary adsorption can be visualized using a z–y diagram, which is for a binary mixture directly linked to the selectivity:

$$S_{CO_2,i} = \frac{z_{CO_2}/z_i}{y_{CO_2}/y_i} \tag{24}$$

z and y are the mole fractions of the two components in the adsorbed and bulk phase, respectively, with i standing for H_2 or N_2. For both mixtures this is shown in Fig. 11 at the same pressures used in Figs. 7 and 8. For the sake of clarity the calculation at 3.0 MPa is not shown as it falls between the two other pressures. All aspects discussed above are summarized in these figures: a very high selectivity of CO_2 compared to H_2 and a smaller one for CO_2 compared to N_2, the overestimation of the H_2 adsorption in the measured data compared to the binary Sips and IAST predictive calculations, the small difference between binary Sips and IAST in the case of CO_2/H_2 and the better description of the experimental data of CO_2/N_2 adsorption using IAST. It is interesting to emphasize that both models, binary Sips and IAST, predict a selectivity dependence on the bulk mole fraction as well as on the adsorption pressure whereas in the experimental values no trend can be observed.

6 Concluding remarks

Measuring the equilibrium adsorption isotherms of the relevant components is one of the first and easiest possibilities to characterize an adsorbent material and to check its suitability for a special application. As shown in the previous sections a lot of information can be obtained from this data and different possibilities exist to obtain the desired parameters. In this paper adsorption data of pure CO_2, N_2 and H_2 on activated carbon at different temperatures between 25 °C and 140 °C and at pressures up to 21.0 MPa are presented and evaluated. The experimental data are described with Langmuir and Sips isotherms by fitting the corresponding parameters to the data. Furthermore, the temperature dependence of the isotherms is taken into account. In a next step different methods to obtain the Henry's constants and isosteric heats are discussed and compared. Experimental binary data of CO_2/H_2 and CO_2/N_2 at 25 °C are compared to predictions using the pure component isotherm parameters. The data is discussed in terms of assessing the suitability of the material for the desired process application and will be used in a detailed process development and optimization to evaluate the potential for pre-combustion CO_2 capture.
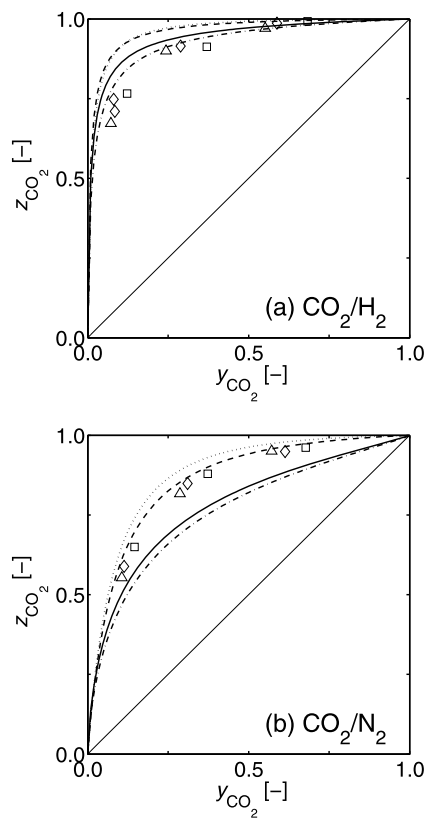
Fig. 11 z–y diagrams for CO_2/H_2 and CO_2/N_2 mixtures at 25 °C and different pressures, *symbols* are experimental points, *lines* represent calculation with binary Sips and IAST using the pure component parameters; 2.0 MPa: *triangles* (experiments), *solid lines* (binary Sips) and *dashed line* (IAST); 3.0 MPa: *diamonds* (experiments); 6.0 MPa (for CO_2/N_2) or 8.0 MPa (for CO_2/H_2): *squares* (experiments), *chain dotted line* (binary Sips) and *dotted line* (IAST)

Appendix: Determination of the weighting factor for isotherm fitting

The weighting factor g_j, that is used for isotherm fitting, accounts for the inhomogeneous distribution of the experimental points by weighting them according to the distance in pressure to the next point resulting in a first estimate of a weighting factor r_j:

$$r_j = p_j - p_{j+1} \quad \text{for all } j = 1, \ldots, N-1 \tag{25}$$

$$r_N = p_N \tag{26}$$

N is the total number of experimental points for one isotherm and the points are listed in a way that the pressure is decreasing, i.e. p_1 is the highest pressure and p_N is the lowest.

However all experimental points at pressures less than 1.5 MPa are weighted 10 times more as this is the region of major interest in further use (compare (27)) which results in a new weighting factor t_j. To make fits of different isotherms comparable the weighting factors for each isotherm are scaled to sum up to 1 as shown in (28), giving the final weighting factor g_j.

$$t_j = 10 r_j \quad \text{for all } j \text{ if } p_j \leq 1.5 \text{ MPa} \tag{27}$$

$$g_j = \frac{t_j}{\sum_{j=1}^{N} t_j} \tag{28}$$

References

Al-Muhtaseb, S.A., Ritter, J.A.: New virial-type model for predicting single- and multicomponent isosteric heats of adsorption. Ind. Eng. Chem. Res. **37**(2), 684–696 (1998)

Do, D.: Adsorption Analysis: Equilibria and Kinetics. Imperial College Press, London (1998), Chap. 3.2.2, pp. 57–64

Dreisbach, F., Staudt, R., Keller, J.: High pressure adsorption data of methane, nitrogen, carbon dioxide and their binary and ternary mixtures on activated carbon. Adsorption **5**, 215–227 (1999)

Gamba, G., Rota, R., Storti, G., Carra, S., Morbidelli, M.: Absorbed solution theory models for multicomponent adsorption equilibria. AIChE J. **35**(6), 959–966 (1989)

Grande, C.A., Lopes, F.V.S., Ribeiro, A.M., Loureiro, J.M., Rodrigues, A.E.: Adsorption of off-gases from steam methane reforming (H_2, CO_2, CH_4, CO and N_2) on activated carbon. Sep. Sci. Technol. **43**(6), 1338–1364 (2008)

Hamon, L., Jolimaitre, E., Pirngruber, G.D.: CO_2 and CH_4 separation by adsorption using cu-btc metal-organic framework. Ind. Eng. Chem. Res. **49**(16), 7497–7503 (2010)

Humayun, R., Tomasko, D.: High-resolution adsorption isotherms of supercritical carbon dioxide on activated carbon. AIChE J. **46**, 2065–2075 (2000)

Hwang, K., Gong, S., Lee, W.: Adsorption equilibria for hydrogen and carbon dioxide on activated carbon at high pressure up to 30 atm. Korean J. Chem. Eng. **8**, 148–155 (1991)

IPCC: IPCC Special Report on Carbon Capture and Storage. Cambridge University Press, Cambridge (2005)

Langmuir, I.: The adsorption of gases on plane surfaces of glass, mica and platinum. J. Am. Chem. Soc. **40**(9), 1361–1403 (1918)

Lopes, F.V.S., Grande, C.A., Ribeiro, A.M., Loureiro, J.M., Evaggelos, O., Nikolakis, V., Rodrigues, A.E.: Adsorption of H_2, CO_2, CH_4, CO, N_2 and H_2O in activated carbon and zeolite for hydrogen production. Sep. Sci. Technol. **44**, 1045–1073 (2009)

Murata, K., El-Merraoui, M., Kaneko, K.: A new determination method of absolute adsorption isotherm of supercritical gases under high pressure with a special relevance to density-functional theory study. J. Chem. Phys. **114**(9), 4196–4205 (2001)

Myers, A.L., Prausnitz, J.M.: Thermodynamics of mixed-gas adsorption. AIChE J. **11**(1), 121–127 (1965)

NIST: NIST Chemistry WebBook (2011). http://webbook.nist.gov/chemistry

Ottiger, S., Pini, R., Storti, G., Mazzotti, M.: Competitive adsorption equilibria of CO_2 and CH_4 on dry coal. Adsorption **14**, 539–556 (2008)

Pan, H., Ritter, J.A., Balbuena, P.B.: Examination of the approximations used in determining the isosteric heat of adsorption from the Clausius Clapeyron equation. Langmuir **14**(21), 6323–6327 (1998)

Park, J.H., Kim, J.N., Cho, S.H., Kim, J.D., Yang, R.T.: Adsorber dynamics and optimal design of layered beds for multicomponent gas adsorption. Chem. Eng. Sci. **53**(23), 3951–3963 (1998)

Pini, R., Ottiger, S., Rajendran, A., Storti, G., Mazzotti, M.: Reliable measurement of near-critical adsorption by gravimetric method. Adsorption **12**(5), 393–403 (2006)

Ruthven, D.: Principles of Adsorption and Adsorption Processes. Wiley, New York (1984)

Ruthven, D., Farooq, S., Knaebel, K.: Pressure Swing Adsorption. VCH, Weinheim (1994)

Shen, C., Grande, C.A., Li, P., Yu, J., Rodrigues, A.E.: Adsorption equilibria and kinetics of CO_2 and N_2 on activated carbon beads. Chem. Eng. J. **160**(2), 398–407 (2010)

Sips, R.: On the structure of a catalyst surface. J. Chem. Phys. **16**(5), 490–495 (1948)

Sips, R.: On the structure of a catalyst surface. II. J. Chem. Phys. **18**(8), 1024–1026 (1950)

Sircar, S.: Excess properties and thermodynamics of multicomponent gas adsorption. J. Chem. Soc. Faraday Trans. **81**, 1527–1540 (1985)

Sircar, S.: Estimation of isoteric heats of adsorption of single gas and multicomponent gas mixtures. Ind. Eng. Chem. Res. **31**(7), 1813–1819 (1992)

Sudibandriyo, M., Pan, Z., Fitzgerald, J.E., Robinson, R.L., Gasem, K.A.M.: Adsorption of methane, nitrogen, carbon dioxide, and their binary mixtures on dry activated carbon at 318.2 K and pressures up to 13.6 MPa. Langmuir **19**(13), 5323–5331 (2003)

Taqvi, S.M., LeVan, M.D.: A simple way to describe nonisothermal adsorption equilibrium data using polynomials orthogonal to summation. Ind. Eng. Chem. Res. **36**(2), 419–423 (1997a)

Taqvi, S.M., LeVan, M.D.: Virial description of two-component adsorption on homogeneous and heterogeneous surfaces. Ind. Eng. Chem. Res. **36**(6), 2197–2206 (1997b)

Xiao, P., Zhang, J., Webley, P., Li, G., Singh, R., Todd, R.: Capture of CO_2 from flue gas streams with zeolite 13X by vacuum-pressure swing adsorption. Adsorption **14**(4), 575–582 (2008)

Yang, R.: Gas Separation by Adsorption Processes. Imperial College Press, London (1997), Chap. 7.2.3, pp. 260–262

Zhou, L.: Adsorption isotherms for the supercritical region. In: Toth, J. (ed.) Adsorption—Theory, Modeling, and Analysis, pp. 211–250. Dekker, New York (2002), Chap. 4